Convolution mixture of FBF and modulated FBF and application to HRTEM images

ZHANGYUN TAN[1], OLIVIER ALATA[2], MAXIME MOREAUD[3], ABDOURRAHMANE M. ATTO[1]

[1] Laboratoire d'Informatique, Systèmes, Traitement de l'Information et de la Connaissance
5 chemin de Bellevue, Polytech Annecy-Chambéry, BP 80439, 74944, Annecy-le-Vieux, France
[2] Laboratoire Hubert Curien, 18 Rue du Professeur Benoît Lauras, 42000, Saint-Etienne, France
[3] IFP Energies Nouvelles, BP 3, 69360, Solaize, France

[1] Zhangyun.Tan@univ-savoie.fr, Abdourrahmane.Atto@univ-savoie.fr
[2]Olivier.Alata@univ-st-etienne.fr, [3]Maxime.Moreaud@ifpen.fr.

Résumé **-** Dans cet article, nous proposons de modéliser certaines textures apparaissant dans les images à Haute Résolution de Microscopie Electronique en Transmission (HRMET) à l'aide d'un mélange composé d'un champ Brownien fractionnaire avec une version modulée d'un tel champ. Le mélange en question est basé sur un opérateur de convolution s'appliquant sur les variables spatiales des deux champs considérés. Nous présentons deux méthodes d'estimation des paramètres de Hurst du modèle en utilisant une approche par ondelettes. Nous présentons également une méthode pour localiser les pôles du modèle. Nous montrons la pertinence de ce modèle en l'appliquant à l'analyse des images HRMET contenant des phases actives d'un catalyseur.

Abstract **-** In this paper, we propose a mixture involving a fractional Brownian field and a modulated version of such a field for modeling High Resolution Transmission Electron Microscopy (HRTEM) textures. The mixture under consideration is defined from the convolution operator applied on spatial variables of the two fields under consideration. We present estimation methods for the parameters of the model (2 Hurst parameters and 2 spectral poles) based on Wavelet Packet (WP) spectrum. The relevance of our method is highlighted by its application to the analysis of HRTEM images with active phases of a catalyst.

1 Introduction

Texture modeling plays an important role in application domains involving image analysis. The main difficulty of texture modeling is in finding a random field model capable of capturing several types of statistical dependencies.

In this paper, we are interested in High-Resolution Transmission Electron Microscopy (HRTEM) textures. More specifically, we are interested in the observation of catalysts microstructures at nanometer scale. With HRTEM micrographs, dark or bright linear patterns (fringes) can be observed and correspond to atomic planes of active phases deposited on a catalyst support (see Figure 1). The selectivity and activity of the catalyst can be linked to some descriptive parameters of the structure characterization [8, 9] as, for instance, the number of fringes per packet, the interlayer spacing values and fringe lengths. We propose to use a model-based approach to characterize these fringes.

Some spatial random processes such as the Fractional Brownian Fields (FBF) have shown efficiency in texture analysis [1, 2, 4, 6 and 7] and texture synthesis [3, 5]. The standard FBF has just one single parameter (Hurst parameter) which is not representative of fringes: it rather corresponds to the image background homogeneity/regularity. To make relevant description of fringes such as those of HRTEM textures, we propose a convolution mixture of an FBF and a modulated FBF.

This work was supported by ARC6-TIC, Rhône-Alpes region, France.

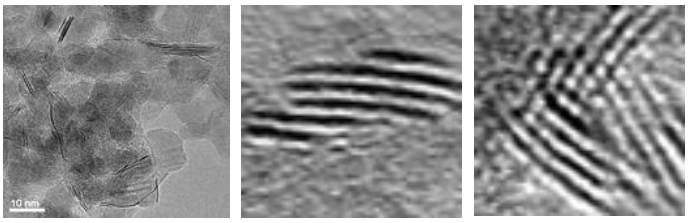

Figure 1: Left, TEM micrographs at high resolution of catalyst with active phases (black fringes) deposited on the support. Middle and Right, zoom on two active phases.

This paper is organized as follows. Section 2 introduces preliminary results on FBF. Section 3 proposes the convolution mixture model and the estimation procedure of its parameters. Section 4 presents the experimental results and highlights the application on HRTEM images. Finally section 5 concludes this paper and gives some prospects.

2 Preliminary results on FBF

2.1 Definition and properties of FBF model

The FBF, noted here as $F_H = \{F_H(x,y),\ (x,y) \in \mathbb{Z}^2\}$, is a zero-mean real valued isotropic random field characterized by a Hurst parameter H, $0 < H < 1$. Its autocorrelation function is

$$R_{F_H}(x,y,s,t) = \frac{\sigma^2}{2}\{(x^2+y^2)^H + (s^2+t^2)^H - ((x-s)^2+(y-t)^2)^H\}, \quad (1)$$

with $(s,t) \in \mathbb{Z}^2$.

The spectrum of FBF is defined by association and can be written as [2]

$$S_{F_H}(u,v) = \xi(H)\frac{1}{(u^2+v^2)^{H+1}} = \xi(H)\frac{1}{\|f\|^{2H+2}}, \quad (2)$$

with $(u,v) \in [-\pi,\pi]^2$, where $\xi(H) = \frac{2^{-(2H+1)}\pi^2\sigma^2}{sin(\pi H)\Gamma^2(1+H)}$, $\|f\| = \sqrt{u^2+v^2}$ and Γ is the gamma function.

From equation (2), the spectrum of FBF has the form,

$$S_{FBF}(u,v) \sim \frac{1}{\|f\|^{\alpha}}. \quad (3)$$

This spectrum thus shows an exponential decay and the following provides the Log-RDWP and Log-RPWP estimation methods for estimating the decay parameter $\alpha = 2\mathrm{H} + 2$.

2.2 Hurst Parameter Estimation of FBF

In the literature, there exist some methods for estimating the Hurst parameter [4, 7]. These methods use log-regression parameter estimation based on periodogram for 1D fractional Brownian motion (fBm). The wavelet packet estimation method has been shown to be more relevant than the periodogram parameter estimation in 1D [2]. Thus we propose, in this paper, the Log-Regression on Diagonal WP spectrum (Log-RDWP) and the Log-Regression on polar representation of WP spectrum (Log-RPWP).

2.2.1 Log-RDWP estimation method

This estimation method relies on the following formula:

$$\hat{\alpha}_{Log\text{-}RDWP} = \frac{1}{C} \sum_{0<j<k\leq N} \frac{\log\left(\frac{\hat{S}_{FBF}(u_j,u_j)}{\hat{S}_{FBF}(u_k,u_k)}\right)}{\log\left(\frac{\|f_k\|}{\|f_j\|}\right)}, \quad (4)$$

where $C = \frac{N!}{2(N-2)!}$ is the number of all possible combinations of the log-ratios, $\hat{S}_{FBF}$ denotes the spectrum estimated from method [2], $\|f\| = \sqrt{u^2+v^2}$, N is the number of considered 2D frequencies, $0 < j \leq N$ and $j < k \leq N$.

2.2.2 Log-RPWP estimation method

The polar estimation method consists in the following steps. In the first step, the spectrum with polar coordinates W_I is computed:

$$W_I(r,\theta) = T\left(\widehat{S_I}(u,v)\right), \quad (5)$$

where $\widehat{S_I}$ is the spectrum estimated from method [2] of the input image with Cartesian coordinates and T is the Cartesian-to-polar transform.
In the second step, averages are done over the angles:

$$P_I(r_i) = \frac{1}{M}\sum_{j=1}^{M} W_I(r_i,\theta_j), \text{with } 1 \leq i \leq N. \quad (6)$$

This procedure can be justified by the isotropy property of the FBF model considered. In the third step, α is estimated by:

$$\hat{\alpha}_{Log\text{-}RPWP} = \frac{1}{C} \sum_{0<i<k\leq N} \frac{log\left(\frac{P_I(r_i)}{P_I(r_k)}\right)}{\log\left(\frac{r_k}{r_i}\right)}, \quad (7)$$

where $C = \frac{N!}{2(N-2)!}$ is the number of all possible combinations of the log-ratios, N is the number of considered radii.

From equation (2), the spectrum of F_H exhibits a singular frequency point located at the zero frequency. The following provides the proposed model.

3 Convolution mixture of FBF and modulated FBF – Parameter estimation

The convolution mixture considered hereafter is derived from the construction given in [3]. This random field construction involves modulation and convolution operators applied on the spatial variables of a sequence of FBF. We first present the modulation of an FBF, its convolution with another FBF and finally, the estimation procedure.

3.1 Modulated FBF

We define a random field Y by setting

$$Y_H(x,y) = F_H(x,y)e^{iu^*x}e^{iv^*y}. \quad (8)$$

The field Y_H is an FBF F_H modulated by a complex exponential wave associated with a frequency point (u^*,v^*) in the grid $[-\pi,\pi]\times[-\pi,\pi]$.

Its autocorrelation function is given by:

$$R_{Y_H}(x,y,s,t) = R_{F_H}(x,y,s,t)e^{iu^*(x-s)}e^{iv^*(y-t)}. \quad (9)$$

The spectrum of Y_H, noted as S_{Y_H}, can be written as:

$$S_{Y_H}(u,v) = S_{F_H}(u-u^*, v-v^*) = \xi(H)\frac{1}{((u-u^*)^2+(v-v^*)^2)^{H+1}}. \quad (10)$$

From equation (10), S_{Y_H} has a singularity at the frequency point (u^*,v^*).

3.2 Convolution of a modulated FBF with an FBF

The convolution mixture, hereafter noted $Z(x,y)$, is defined as the convolution of the FBF field F_{H_1} and the modulated FBF Y_{H_2}.

$$Z(x,y) = F_{H_1} * Y_{H_2}(x,y), \quad (11)$$

where F_{H_1} is a standard FBF with Hurst parameter H_1 and a pole located at (0,0) (see Eq. (2)), and Y_{H_2} is a modulated FBF with Hurst parameter H_2 and a pole located at (u^*,v^*).

The spectrum of Z, denoted $S_Z(u,v)$, can be written as:

$$S_Z(u,v) = S_{F_{H_1}}(u,v)\, S_{Y_{H_2}}(u,v) = \frac{\xi(H_1)}{(u^2+v^2)^{H_1+1}}\frac{\xi(H_2)}{((u-u^*)^2+(v-v^*)^2)^{H_2+1}}. \quad (12)$$

This spectrum shows 2 poles located at (0,0) and (u^*,v^*) respectively.

3.3 Estimation procedure

In this section, we present the procedure to estimate the Hurst parameters of the proposed model. First, we estimate the parameter H_1 of the standard FBF (first component of the mixture), and then we estimate the parameter H_2 of the modulated FBF (second component of the mixture).

For estimating H_1, we use the method described in Section 2.2 by focusing on a neighborhood of frequency (0,0). The estimation of H_2 is performed in two steps: first, we remove the contribution of the FBF with parameter H_1 (see Eq. (14)). The residual spectrum has one single pole with exponential decay characterized by H_2. We seek the maximum of the power spectral density and locate this pole. We translate (demodulation) this pole to the zero frequency point and thus get one single pole located at zero frequency similar to the case of a standard FBF. We then estimate H_2 by using the method given in Section 2.2.

4 Experimental results and application on HRTEM images

4.1 Experimental results

In this section, we present estimation results for the Hurst parameters H_1 and H_2 of the mixture of FBF.

Table 1: Mean values of estimated $\alpha = 2H_1 + 2$ and variances.

Size Image	512*512								2048*2048							
Real Value	2,4		2,8		3,2		3,6		2,4		2,8		3,2		3,6	
Estimated	α	Var(α)	α	Var(α)	α	Var(α)	α	Var(α)	α	Var(α)	α	Var(α)	α	Var(α)	α	Var(α)
RDWP_8	1,781	0,145	2,132	0,160	2,651	0,424	3,236	0,292	2,308	0,023	**2,801**	0,035	3,190	0,029	3,727	0,014
RDWP_12	2,186	0,038	2,553	0,086	2,993	0,053	3,553	0,090	2,482	0,004	2,949	0,013	3,337	0,009	3,833	0,005
RDWP_16	1,833	0,039	2,293	0,031	2,772	0,044	3,343	0,039	2,241	0,004	2,748	0,008	**3,193**	0,007	3,642	0,001
RDWP_20	2,197	0,039	2,612	0,007	3,035	0,030	3,542	0,037	**2,401**	0,010	2,898	0,009	3,329	0,012	3,760	0,008
RDWP_24	2,145	0,045	2,688	0,019	3,050	0,019	3,510	0,018	2,339	0,001	2,842	0,003	3,278	0,004	3,725	0,004
RDWP_28	2,074	0,021	2,693	0,011	3,066	0,010	3,483	0,025	2,322	0,002	2,834	0,002	3,282	0,002	3,733	0,002
RDWP_32	1,935	0,009	2,523	0,007	2,987	0,025	3,400	0,014	2,195	0,004	2,709	0,003	3,153	0,004	3,615	0,009
RDWP_64	1,778	0,008	2,487	0,006	2,936	0,006	3,433	0,002	1,835	0,001	2,510	0,003	3,048	0,002	3,562	0,003
RPWP_8	2,649	0,026	3,133	0,056	3,594	0,081	4,138	0,023	2,688	0,010	3,209	0,009	3,701	0,015	4,260	0,007
RPWP_12	2,501	0,017	2,947	0,035	3,398	0,029	3,895	0,010	2,554	0,003	3,070	0,004	3,543	0,004	4,012	0,002
RPWP_16	2,486	0,004	2,948	0,016	3,435	0,018	3,942	0,003	2,542	0,001	3,060	0,001	3,523	0,002	3,997	0,001
RPWP_20	2,441	0,004	2,906	0,007	3,363	0,008	3,860	0,003	2,498	0,001	3,011	0,001	3,462	0,001	3,940	0,001
RPWP_24	**2,377**	0,002	2,875	0,005	3,335	0,006	3,799	0,002	2,440	0,001	2,953	0,001	3,402	0,001	3,872	0,001
RPWP_28	2,322	0,002	2,844	0,003	3,312	0,005	3,767	0,002	2,398	0,001	2,919	0,001	3,377	0,001	3,841	0,001
RPWP_32	2,282	0,001	**2,819**	0,002	**3,298**	0,004	3,746	0,001	2,346	0,001	2,892	0,001	3,357	0,001	3,819	0,001
RPWP_64	1,842	0,001	2,544	0,001	3,081	0,001	**3,584**	0,001	1,885	0,001	2,570	0,001	3,114	0,001	**3,607**	0,001

Table 2: Mean values of estimated $\alpha = 2H_2 + 2$ and variances.

Size Image	512*512								2048*2048							
Real Value	2,4		2,8		3,2		3,6		2,4		2,8		3,2		3,6	
Estimated	α	Var(α)	α	Var(α)	α	Var(α)	α	Var(α)	α	Var(α)	α	Var(α)	α	Var(α)	α	Var(α)
RDWP_8	1,706	0,078	2,021	0,230	2,668	0,281	2,921	0,043	2,259	0,039	2,639	0,018	3,069	0,043	3,645	0,031
RDWP_12	1,837	0,112	2,348	0,097	2,866	0,135	3,114	0,067	2,347	0,012	2,782	0,010	3,252	0,009	3,779	0,006
RDWP_16	1,712	0,049	2,195	0,043	2,711	0,044	3,147	0,038	2,180	0,012	2,648	0,017	3,082	0,009	3,575	0,007
RDWP_20	1,898	0,031	2,452	0,018	3,022	0,019	3,461	0,031	2,252	0,008	2,757	0,003	3,212	0,004	3,702	0,007
RDWP_24	2,075	0,023	2,525	0,014	3,165	0,009	3,512	0,028	2,310	0,005	2,820	0,001	3,305	0,002	3,793	0,002
RDWP_28	2,088	0,016	2,565	0,020	3,183	0,012	3,533	0,035	2,303	0,006	2,831	0,002	3,326	0,002	3,790	0,003
RDWP_32	1,904	0,013	2,376	0,014	2,990	0,019	3,373	0,020	2,156	0,002	2,720	0,004	3,180	0,001	3,666	0,002
RDWP_64	1,557	0,008	2,363	0,014	2,947	0,008	3,388	0,010	1,705	0,006	2,459	0,002	3,030	0,003	3,535	0,003
RPWP_8	2,345	0,118	2,878	0,103	3,735	0,080	3,944	0,065	2,521	0,021	3,084	0,009	3,703	0,024	4,286	0,030
RPWP_12	2,195	0,040	2,725	0,030	3,471	0,058	3,663	0,035	2,420	0,011	2,966	0,003	3,506	0,012	4,030	0,013
RPWP_16	2,230	0,025	2,785	0,015	3,453	0,027	3,824	0,012	2,432	0,005	2,979	0,002	3,496	0,009	4,025	0,005
RPWP_20	2,256	0,015	2,783	0,008	3,414	0,018	3,839	0,009	2,408	0,004	2,956	0,002	3,467	0,004	3,972	0,003
RPWP_24	2,191	0,012	2,763	0,006	3,338	0,009	3,778	0,006	2,350	0,004	2,907	0,001	3,401	0,003	3,889	0,002
RPWP_28	2,184	0,010	2,752	0,004	3,312	0,009	3,774	0,005	2,311	0,003	2,882	0,001	3,375	0,002	3,860	0,001
RPWP_32	2,119	0,009	2,715	0,003	3,281	0,006	3,725	0,005	2,255	0,003	2,854	0,001	3,346	0,001	3,834	0,001
RPWP_64	1,737	0,004	2,485	0,001	3,088	0,001	3,589	0,000	1,816	0,001	2,555	0,000	3,116	0,000	3,626	0,000

In table 1 and 2, RDWP_N and RPWP_N mean that α is estimated by the Log-RDWP method and Log-RPWP estimation method, respectively, where N is the number of samples (see Eq. 4 & 7). In table 2, the location of the pole (u^*, v^*) is assumed to be known. We use the Daubechy filter for computing the WP spectrum. In order to evaluate the performance of the Log-RDWP and Log-RPWP estimation methods, we generate 10 realizations of an FBF for $\alpha \in \{2.4, 2.8, 3.2, 3.6\}$ and for two different image sizes: 512×512 and 2048×2048. Tables 1 and 2 give estimation results for H_1 and H_2 Hurst parameters. Best results are highlighted in red.

From the results presented in the Tables 1 and 2, we find that, for small size images, the Log-RPWP method yields more relevant estimation of α parameter than the Log-RDWP method. For images with a large size, the Log-RDWP method gives comparable results to those of the Log-RPWP method.

We present now the experimental results for localizing the pole (u^*, v^*). The pole localization is computed from the maximum of the power spectral density estimated using WP spectrum. The accuracy of the maximum spectrum to indicate the location of the pole is given in Table 3.

Table 3: Mean values of estimated (u^*, v^*) and their variances computed from Monte-Carlo simulations on 10 modulated FBF realizations with image size equal to 512×512.

True Value		H	Etimator		Var(Etimator)	
U	V		U	V	U	V
0,7854	0,3927	0,2	0,7854	0,3902	0	0,0001
		0,4	0,7805	0,3927	0,0001	0
		0,6	0,7829	0,3927	0,0001	0
		0,8	0,7805	0,3927	0,0001	0
0,3927	0,1963	0,2	0,3927	0,1963	0	0
		0,4	0,3927	0,1963	0	0
		0,6	0,3878	0,1767	0,0002	0,0039
		0,8	0,3927	0,1963	0	0
0,1963	0,0982	0,2	0,1963	0,0785	0	0,0009
		0,4	0,1767	0,0589	0,0039	0,0010
		0,6	0,1571	0,0810	0,0069	0,0001
		0,8	0,1571	0,0638	0,0069	0,0012

The following proposes the use of this mixture model for analyzing HRTEM texture.

4.2 HRTEM texture analysis

Let us denote now one HRTEM image as

$$I = \{I(x, y)\}. \qquad (13)$$

The image I is considered as a finite realization of the random field Z (see Section 3). The mixture of FBF has a spectral representation associated with two peaks: one peak located at zero frequency and the other located elsewhere. The peak at the zero frequency corresponds to slow grey-level variations in the HRTEM image (considered as background) and will be modeled by an FBF. Fundamentally, this peak is not interesting to characterize the active phase (fringes in the HRTEM image). We thus use a modulated FBF to model fringes.

Let us denote S_I as the wavelet packet spectrum of I. The image characterization procedure from the convolution mixture model presented above can be written as follows. In the first step, we estimate the Hurst parameter H_1 from S_I (first FBF of the mixture with zero-pole). The associated field represents the image background. Parameter H_1 informs us on the

regularity of this background. In the second step, we remove the contribution of the first FBF in *I*. We obtain the residual spectrum given by

$$S_{residual}(u,v) = \frac{S_I(u,v)}{S_{FBF}(u,v)}. \qquad (14)$$

This residual is associated to the second FBF of the mixture model (the fringes). Finally, we estimate the Hurst parameter H_2 involved in the residual: for this purpose, we locate the maximum of the power spectral density of the residual, we shift this maximum to zero frequency (demodulation step) and we estimate H_2 from polar log WP spectrum regression (see Section 3.3).

Spectra of HRTEM images mostly show a significant peak at the zero frequency and an exponential decay in the neighborhood of this peak. This has been emphasized in Figure 2 by providing the WP spectrum of the HRTEM images. Each row of Figure 2 is associated to one HRTEM image. For each line, from left to right, we present the initial HRTEM image, its WP spectrum, its WP spectrum after removing the zero-pole FBF part from the initial WP spectrum and the two Hurst parameters estimated from the HRTEM image. The position of the second pole informs us about orientation, and periodicity (thickness) of the fringes. The value of H_2 may give us some information about the spatial distortion of active phase structure.

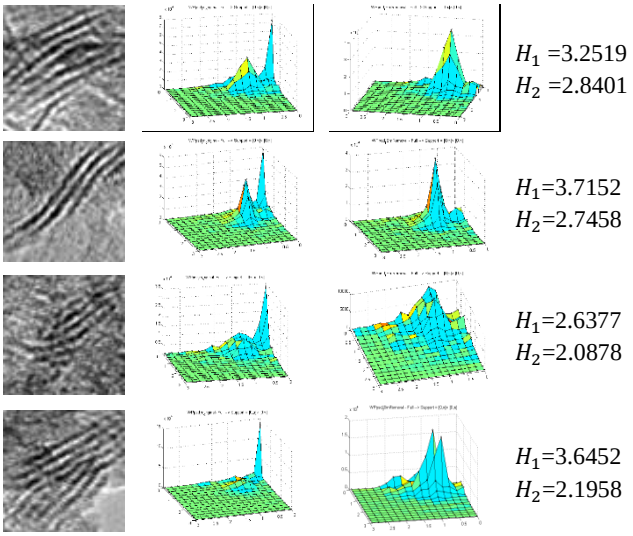

Figure 2: Texture analysis of HRTEM images

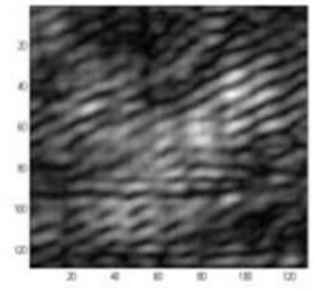

Figure 3: Texture synthesis from the HRTEM image of Figure 3 top-left using the mixture of two factors FBF with parameters H_1=3.2519 and H_2=2.8401.

Figure 3 gives one example of texture synthesis from HRTEM image. The synthesized texture presents some structural similarities with the original HRTEM image.

5 Conclusion

In this paper, we have proposed : *i)* a convolution mixture model composed by a Fractional Brownian Field and its modulated version, *ii)* two estimation methods for the Hurst parameters of the model in 2D (Log-RDWP and Log-RPWP) and *iii)* the application of the mixture FBF model to characterize HRTEM images. The mixture of FBF model has a spectral representation associated with two peaks and two Hurst parameters H_1 and H_2. Its peak located at zero frequency characterizes the background through its Hurst parameter H_1 and the second peak is representative to fringes with a stochastic regularity parameter H_2.

In future work, we will investigate the case of heterogeneous HRTEM fringes: these fringes may require a mixture with a higher number FBF convolution factors so as to take into account several spectral peaks.

6 References

[1] P. Flandrin, "On the spectrum of fractional Brownian Motions", IEEE Transaction on Information Theory, Vol. 35, No. 1, Jan. 1989

[2] A. Atto, Y. Berthoumieu, and P. Bolon, "2-d wavelet packet spectrum for texture analysis", Image Processing, *IEEE*, vol. 22, no. 6, pp. 2495-2500, 2013.

[3] A. M. Atto, Z. Tan, O. Alata and M. Moreaud, "Non-Stationary Texture Synthesis from Random Field Modeling", *IEEE ICIP*, Paris, France, Oct. 2014

[4] B. Pesquet-Popescu and J. L. Véhel, "Stochastic fractal models for image processing", *IEEE Signal Processing Magazine*, vol. 19, no.5, pp.48-62, 2002

[5] B. Pesquet-Popescu and J.C. Pesquet, "Synthesis of bi-dimensional α-stable models with long-range dependence", *Signal Processing*, Elsevier, vol. 82, no. 12, pp. 1927-1940, 2002.

[6] D. P. Kroese and Z. I. Botev, "Spatial process generation", *Lectures on Stochastic Geometry*, Vol.2, Berlin, 2013.

[7] G. Rilling, P. Flandrin and P. Gonçalvès, "Empirical Mode Decomposition, Fractional Gauss Noise and Hurst Exponent Estimation", *IEEE*, 2005

[8] L. Sorbier, A.S. Gay, A. Fécant, M. Moreaud and N. Brodusch, "Measurement of palladium crust thickness on catalysts by optical microscopy and image analysis", *Microscopy and Microanalysis*, 2013

[9] M. Moreaud, D. Jeulin, V. Morard and R. Reval, "TEM image analysis and modeling: application to boehmites nanoparticles", *Journal of Microscopy*, Vol. 245, Pt 2, pp. 186–199, 2012